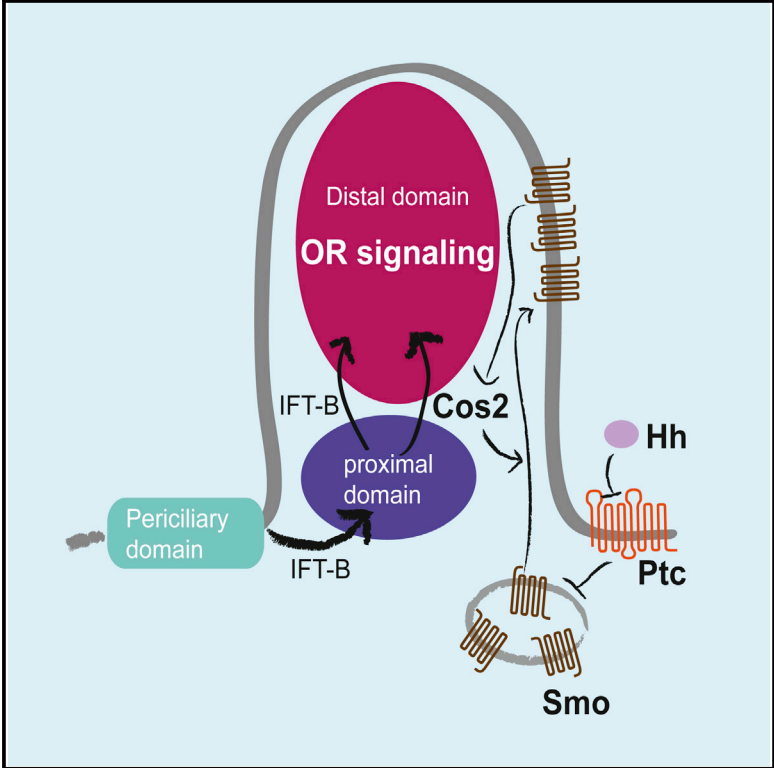


Hedgehog Signaling Regulates the Ciliary Transport of Odorant Receptors in *Drosophila*

Graphical Abstract



Authors

Gonzalo M. Sanchez, Liza Alkhori, Eduardo Hatano, ..., Shadi Jafari, Björn Granseth, Mattias Alenius

Correspondence

mattias.alenius@liu.se

In Brief

Odor responses are tuned to the ambient odorant environment. Sanchez et al. examine the molecular mechanisms that govern the odorant response, and they find that Hedgehog signaling in *Drosophila* regulates localization of the odorant receptors to the cilium compartment.

Highlights

- Hedgehog signaling regulates the odorant response
- Hedgehog signaling controls OR entry and transport within the cilium compartment
- The regulation of OR transport is a cilium-mediated Hedgehog pathway
- Cos2, a Hedgehog-regulated atypical kinesin, localizes ORs within the cilium



Hedgehog Signaling Regulates the Ciliary Transport of Odorant Receptors in *Drosophila*

Gonzalo M. Sanchez,^{1,3} Liza Alkhori,^{1,3} Eduardo Hatano,¹ Sebastian W. Schultz,^{1,2} Anujaianthi Kuzhandaivel,^{1,4} Shadi Jafari,¹ Björn Granseth,¹ and Mattias Alenius^{1,*}

¹Department of Clinical and Experimental Medicine, Linköping University, 58185 Linköping, Sweden

²Present address: Department of Biochemistry, Institute for Cancer Research, Oslo University Hospital–The Norwegian Radium Hospital, 0379 Oslo, Norway

³Co-first author

⁴Present address: Department of Anatomy and Cell Biology, University of Illinois, Chicago, IL 60612, USA

*Correspondence: mattias.alenius@liu.se

<http://dx.doi.org/10.1016/j.celrep.2015.12.059>

This is an open access article under the CC BY-NC-ND license (<http://creativecommons.org/licenses/by-nc-nd/4.0/>).

SUMMARY

Hedgehog (Hh) signaling is a key regulatory pathway during development and also has a functional role in mature neurons. Here, we show that Hh signaling regulates the odor response in adult *Drosophila* olfactory sensory neurons (OSNs). We demonstrate that this is achieved by regulating odorant receptor (OR) transport to and within the primary cilium in OSN neurons. Regulation relies on ciliary localization of the Hh signal transducer Smoothened (Smo). We further demonstrate that the Hh- and Smo-dependent regulation of the kinesin-like protein Cos2 acts in parallel to the intraflagellar transport system (IFT) to localize ORs within the cilium compartment. These findings expand our knowledge of Hh signaling to encompass chemosensory modulation and receptor trafficking.

INTRODUCTION

In both vertebrates and insects, chemical stimuli are detected by odorant receptors (ORs) located on the olfactory sensory neuron (OSN) cilia (DeMaria and Ngai, 2010; Vosshall and Stocker, 2007). Each OSN typically expresses one OR from a large genomic repertoire (Couto et al., 2005; Fishilevich and Vosshall, 2005). The odorant response must be adjusted appropriately to changes in the environment to elicit a suitable behavior and warrant survival of the animal. In *Drosophila*, the type and level of the expressed receptor determine the odorant response (Dobritsa et al., 2003). However, the mechanisms that regulate the receptor level and the level of odorant response are not well understood.

Hedgehog (Hh) signaling regulates nociceptive responsiveness (Babcock et al., 2011). Hh was initially described as a morphogen that defines the segmentation and patterning of the *Drosophila* embryo (Briscoe and Théron, 2013; Goetz and Anderson, 2010). Hh ligand binding to the inhibitory receptor Patched (Ptc) stabilizes the seven-transmembrane protein

Smoothened (Smo) (Denef et al., 2000), which, in vertebrates, translocates to the primary cilium (Corbit et al., 2005) and switches the function of the Gli transcription factors from repression to activation of the Hh target genes (Briscoe and Théron, 2013; Goetz and Anderson, 2010; Ingham et al., 2011; Rohatgi and Scott, 2007; Teperino et al., 2014). The cells that respond to Hh during *Drosophila* development are non-ciliated, which has led to the general view that *Drosophila* and vertebrates have different Hh pathways (Goetz and Anderson, 2010). However, we have demonstrated recently that cilia do mediate the Hh signal in OSNs, one of the few ciliated cell types in *Drosophila* (Kuzhandaivel et al., 2014).

Here, we examine the function of cilium-mediated Hh signaling in *Drosophila* and show that *Smo* knockdown results in a reduced behavioral response to odors. We demonstrate that the level of Hh pathway activity controls the magnitude of the OSN odorant response and regulates the cilium transport of the ORs. Last, we reveal that Smo and the kinesin-like protein Cos2 control OR transport to and within the cilium compartment.

RESULTS

Hh Signaling Regulates the Odorant Response

To investigate the function of the cilium-mediated Hh pathway in *Drosophila* OSNs, we used RNAi to selectively knock down *Smo* in OSNs. Olfactory performance was measured using a set of T-maze behavioral assays. The results showed that flies with OSNs deficient in Smo function (*peb-Gal4 > Smo-inverted repeat (IR)*) were less attracted to vinegar compared with control flies (*Peb-Gal4*) versus *Smo-IR*, Figure 1A). The loss of attraction was not due to a change in motility, as determined by a climbing assay (Figure S1), which indicates that Hh signaling modulates olfaction in *Drosophila*.

To determine whether the change in the behavioral response corresponded to a change in OSN function, we recorded odor-induced changes in intracellular Ca²⁺ concentration in OSNs expressing the genetically encoded fluorescent Ca²⁺ reporter GCAMP5. We initially investigated the response to ethyl acetate, which activates several ORs and OSN classes. In control flies, ethyl acetate triggered robust fluorescence transients that

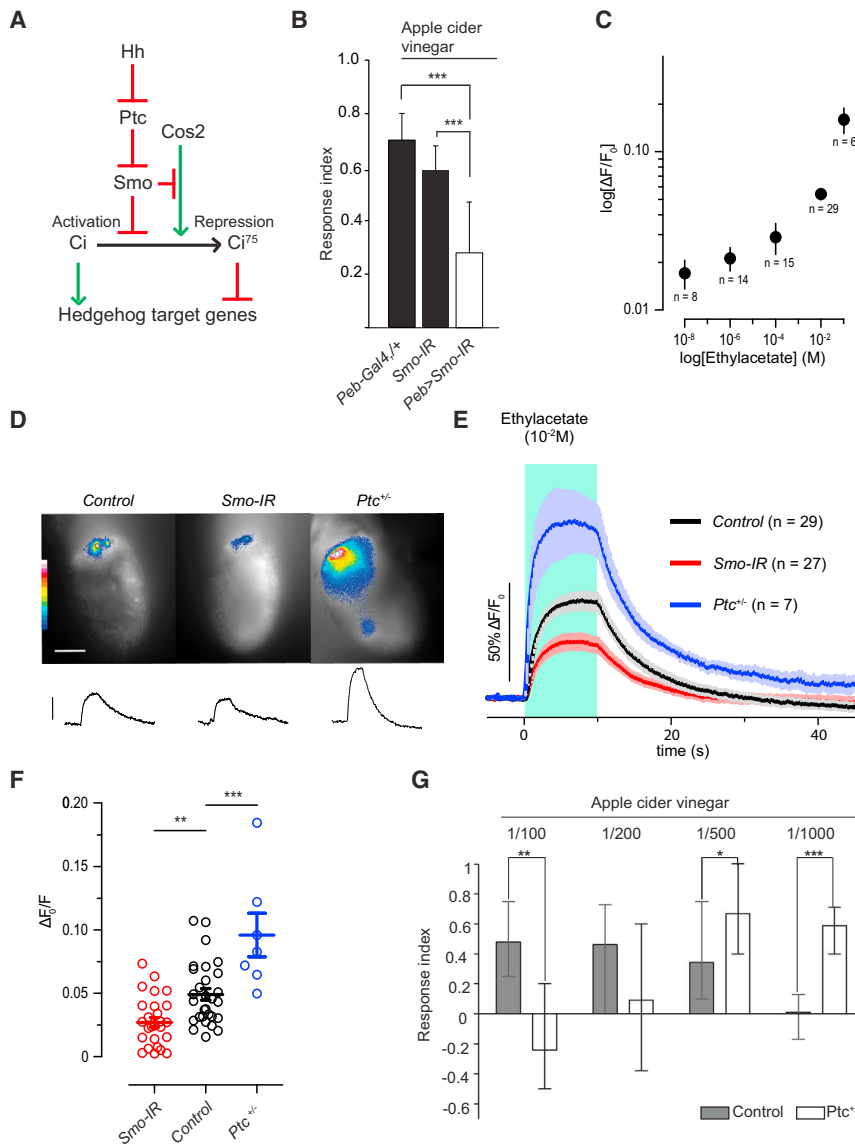


Figure 1. Hh Signaling Modulates the Odorant Response

(A) A model depicting the core Hh pathway. (B) The odorant-evoked behavioral response to apple cider vinegar from the control (*peb-Gal4*, *UAS-Dcr2/+*) flies was calculated as a response index. The RNAi produced by the expression of an inverted repeat (–IR) of *Smo* (*peb-Gal4*, *UAS-Dcr2*; *UAS-Smo-IR*) reduced the flies' response to vinegar. ****p* ≤ 0.001. See also Figure S1. (C) A dose-response plot shows the maximum Ca²⁺ responses evoked in control flies (*peb-Gal4*, *UAS-Dcr2*; *UAS-GCAMP5G*) as a function of ethyl acetate concentration. (D) The representative false color-coded pattern of maximum Ca²⁺ responses evoked by ethyl acetate in control, *Smo-IR* and *Ptc*^{+/-} antennae. (E) The traces represent the averages ± SEM of the ethyl acetate-evoked response from each group. The shaded box indicates the stimulation interval. (F) Scatterplot of the maximum fluorescence intensity measured during ethyl acetate stimulation of control, *Smo-IR*, and *Ptc*^{+/-} antennae (bar graphs denote mean ± SEM). ***p* ≤ 0.01, ****p* ≤ 0.001. See also Figures S2 and S3. (G) The odorant-evoked behavioral response to apple cider vinegar of control and *Ptc*^{+/-} flies. **p* ≤ 0.05, ***p* ≤ 0.01, ****p* ≤ 0.001. See also Figure S1.

increased in magnitude with odor concentration ($\Delta F/F_0 = 49.2\% \pm 4.6\%$, $n = 29$; Figures 1C and 1D). This fluorescence response was attenuated visibly in *Smo* knockdown flies ($\Delta F/F_0 = 27.1\% \pm 3.9\%$, $n = 27$, $p < 0.05$; Figure 1E). In addition, we recorded the fluorescence response to apple cider vinegar, which activates a partially overlapping set of ORs and OSN classes. Again the *Smo* knockdown flies showed a reduced fluorescence response (Figure S2A), which indicates the Hh pathway is a general regulator of the odorant response.

To analyze whether *Ptc*, which inhibits *Smo*, also suppresses the odor response, we performed calcium imaging in heterozygote *Ptc* mutant (*Ptc*^{+/-}) flies. We found that fluorescence responses to ethyl acetate were enhanced dramatically in *Ptc*^{+/-} flies ($\Delta F/F_0 = 96.0\% \pm 17.2\%$, $n = 7$, $p < 0.05$; Figures 1E, 1F, and S3). Similar results were observed when vinegar was used as the stimulant (Figure S2A), showing that *Ptc* and the Hh

pathway generally restrict OSN responsiveness. Behavior analysis of *Ptc*^{+/-} flies revealed sensitized responses with an extended receptive range to vinegar compared with control flies (Figure 1G). Together, our behavioral analysis and calcium imaging recordings demonstrate that the level of activity in the Hh pathway sets OSN odorant response magnitude.

Hh Signaling Regulates OR Cilium Localization

Methyl octanoate activates a single odorant receptor, Or22a (Galizia et al., 2010; Hallem and Carlson, 2006). Our calcium imaging analysis showed a marked loss of methyl octanoate response in *Smo-IR* and a gain of response in *Ptc*^{+/-} flies (Figure S2B), demonstrating that Hh regulates a single OSN class and receptor. To investigate how *Smo* and Hh signaling control the odor response, we analyzed Or22a expression and localization in *Hh* and *Smo* knockdown flies. There were no differences in the number of Or22a-positive OSNs between the control and *Hh* or *Smo* knockdown flies (Figures 2C–2E), showing that the loss of odor response was not due to the loss of OR expression. However, there was a marked reduction in the number of Or22a-positive cilia in *Hh* and *Smo* knockdown flies relative to control flies (Figures 2A and 2B). In addition, a detailed analysis of Or22a localization showed that, in *Smo* and *Hh* knockdowns, the staining occupied the entire cilium compartment rather than the discrete distal localization found in control flies (Figures 2F and

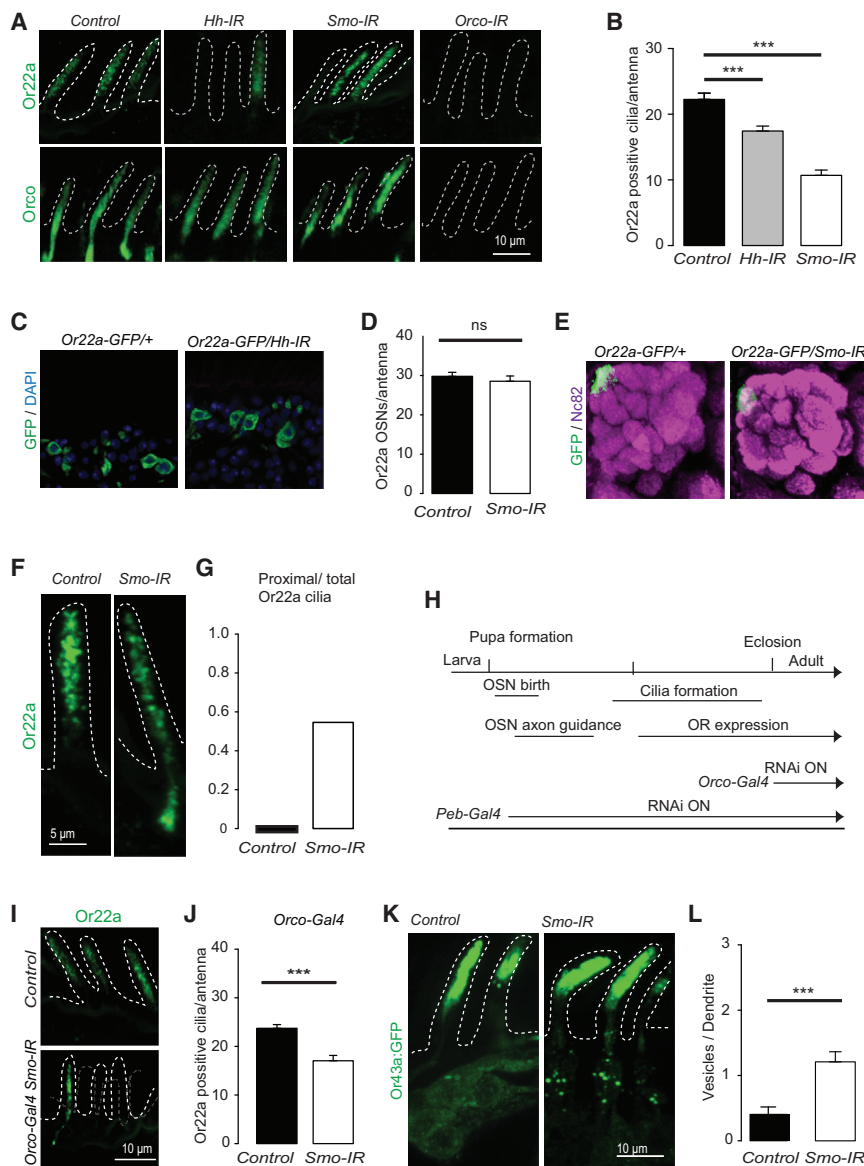


Figure 2. Hh Signaling Regulates Ciliary OR Localization

(A) Normal ciliary localization of Or22a (green, top) requires *Hh*, *Smo*, and *Orco* (*Hh*, *Smo-IR*, and *Orco-IR*) expression. *Orco* (green, bottom) transport is unperturbed in *Hh-IR* and *Smo-IR* flies. The dotted lines outline the sensilla.

(B) Loss of Or22a-positive cilia in *Hh-IR* ($n = 30$) and *Smo-IR* ($n = 15$) compared with control ($n = 34$) flies. *** $p \leq 0.01$.

(C) *OR22a-CD8:GFP* (GFP, green) expression in *Hh-IR* and control flies (nuclei are visualized with DAPI (blue)).

(D) Quantification of GFP-expressing OSNs in control ($n = 10$) and *Smo-IR* ($n = 8$) flies demonstrating that the number of Or22a OSNs is unaltered. ns, not significant.

(E) The Or22a-expressing OSNs show unperturbed axon targeting to the DM2 glomerulus in *Smo-IR* and control flies. (Nc82, magenta, marks neurophil).

(F) Or22a localizes to the distal cilium segment in control and *Smo* knockdown flies to both the distal and proximal segment.

(G) Quantification showing a marked increase in the number of cilia with proximal staining in *Smo* knockdown flies.

(H) Schematic of OSN development, with the onset of *Peb-Gal4* and *Orco-Gal4* expression outlined.

(I) Loss of Or22a (green) ciliary localization in *Orco-Gal4/Smo-IR* flies.

(J) Loss of Or22a-positive cilia in *Orco-Gal4<Smo-IR* compared with control flies ($n = 22$). *** $p \leq 0.01$.

(K) Or43a:GFP forms puncta in the dendrite and cell body of *Smo-IR* OSNs.

(L) Quantification of the increased number of puncta per dendrite in *Smo-IR* flies (control, $n = 40$; *Smo-IR*, $n = 43$). *** $p < 0.001$. Bar graphs show mean \pm SEM.

See also Figure S4.

2G). These results suggest that the Hh pathway regulates transport of Or22a within the cilium.

ORs require the OR coreceptor (*Orco*) for ciliary localization, stability, and function (Figures 2A and S2C; Benton et al., 2006), and initiation of *Orco* expression marks the final step of OSN development (Figure 2H; Jana et al., 2011). Localization of *Orco* within the soma, dendrite, and cilium compartment of OSNs was similar in control and *Smo* knockdown flies (Figure 2A), demonstrating that ciliary structure and transport of *Orco* is intact in knockdown flies. To validate that the Or22a phenotype is not a defect of OSN development and cilium formation, we limited *Smo* knockdown to mature OSNs with *Orco-Gal4*. We found that even this temporally restricted expression of *Smo-IR* produced a loss of Or22a-positive cilia (Figures 2I and 2J), demonstrating that *Smo* regulates OR ciliary localization in mature OSNs.

To better visualize OR transport, we expressed *Or43a:GFP* in all OSNs. Or43a:GFP is a functional OR and localizes to cilia (Figure 2K; Benton et al., 2006). In control fly antennae, Or43a:GFP produced staining in the cilia, soma, and dendrites with few puncta (Figure 2K). In *Smo* knockdown flies, the Or43a:GFP puncta increased in number (Figures 2K and 2L). The puncta were found in all different OSN lineages and types, which suggests that Hh signaling regulates OR transport and the odorant response in most, if not all, OSNs. We further observed that strong overexpression of *Or43a:GFP* rescued the cilium transport phenotype of *Smo-IR* (Figure 2K), implying that Hh-regulated OR transport can be saturated. Next, we mapped the origin of the puncta with a variety of antibodies and found co-localization with the recycling endosome marker Rab11 (Figure S4). Rab11 transports protein to the primary cilia in vertebrates (Knödler et al., 2010; Wang and Deretic, 2015). Our results therefore

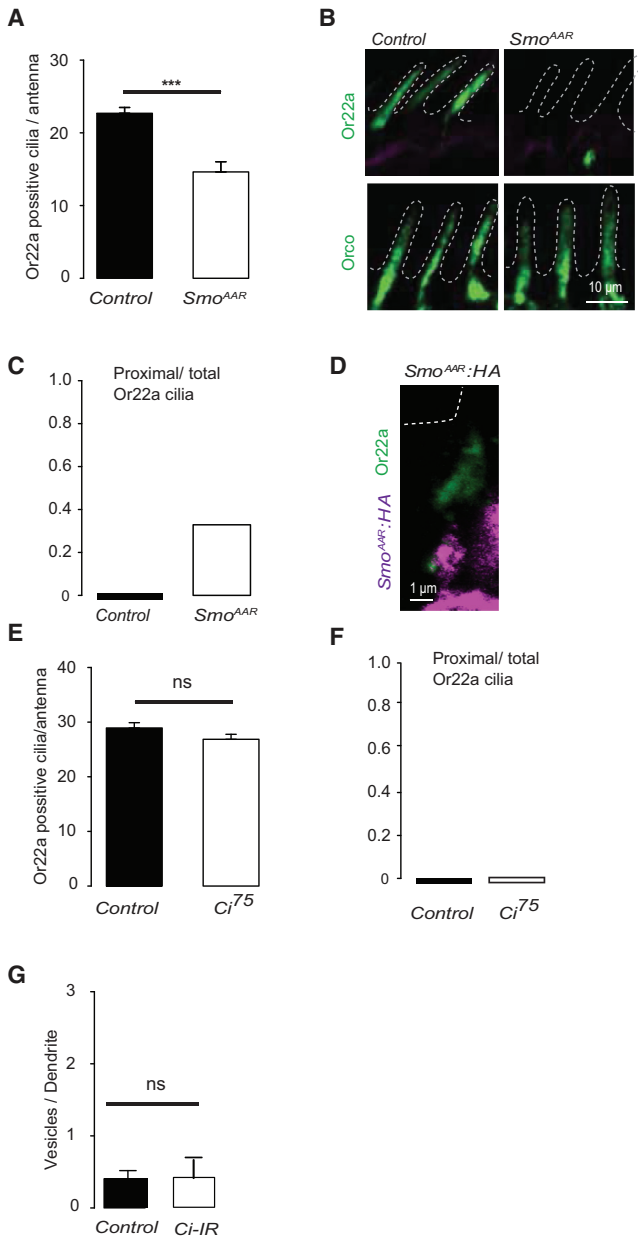


Figure 3. Ciliium Localization of Smo Is Required for OR Ciliium Transport

(A) Expression of the cilia localization mutant *Smo^{AAR}* reduces the number of Or22a-expressing cilia compared with the control (n = 16). ***p < 0.001. (B) Localization of Or22a (top) and Orco (bottom) in control and *Smo^{AAR}* OSNs. (C) Quantification showing a marked increase of Or22a cilia with proximal staining in *Smo^{AAR}* OSNs (n = 12). (D) Or22a (green) and HA (magenta) staining showing that *Smo^{AAR}:HA* does not overlap with the proximal Or22a staining. (E and F) Expression of *Ci⁷⁵* does not reduce the number of Or22a-expressing cilia (E, n = 46, p = 0.636) or the ciliary localization of Or22a (F) compared with the control (n = 30). (G) In *Ci* knockdown flies, the number of puncta was comparable with the number of puncta in control flies (n = 42). Bar graphs show mean ± SEM.

suggest that Hh signaling regulates transport to and within the cilium and that the puncta are vesicles of ORs available for entry into the ciliary compartment.

OR Transport Is Regulated by a Cilium-Mediated Hh Pathway

Thus far, our results show that Hh signaling regulates OR location, but the mechanism remains unclear. We have shown previously that Smo signaling in the OSNs requires localization to the cilia (Kuzhandaivel et al., 2014). Smo has, C-terminal to the last transmembrane region, a hydrophobic and basic residue motif that functions as a ciliary localization motif. Replacement of the first two N-terminal amino acids of the motif (WKR) with alanine (AAR) disrupts the targeting of Smo to the cilia in both vertebrates and *Drosophila* (Corbit et al., 2005; Kuzhandaivel et al., 2014). To address whether ciliary localization of Smo is required to regulate OR transport, we expressed *Smo^{AAR}* in OSNs. Interestingly, *Smo^{AAR}* expression mimicked the *Smo* knockdown phenotype, with a reduced number of Or22a-positive cilia, unperturbed Orco transport, and altered OR ciliary localization (Figures 3A–3D). Therefore, ciliary localization of Smo is part of the mechanism that regulates OR transport.

We have also shown previously that mature OSNs have a canonical Hh pathway that regulates the expression of the Hh target gene *Engrailed* (Kuzhandaivel et al., 2014). Hh target genes are regulated by the transcription factor *cubitus interruptus* (Ci/Gli in vertebrates) (Aza-Blanc et al., 1997; Méthot and Basler, 1999; Ohlmeyer and Kalderon, 1997). In the absence of Hh signaling, Ci is partially degraded to *Ci⁷⁵*, which functions as a transcriptional repressor of Hh target genes (Aza-Blanc et al., 1997). To determine whether *Ci* regulates the expression of the OR transport machinery, we either knocked down *Ci* or expressed *Ci⁷⁵* in OSNs. Interestingly, the Or22a protein localization and number of Or22a-positive cilia in *Ci⁷⁵* OSNs were comparable with the control (Figures 3E and 3F). In addition, the numbers of Or43a vesicles were comparable in *Ci* knockdown and control flies (Figure 3G). The lack of an abnormal phenotype upon *Ci* knockdown or expression of *Ci⁷⁵* indicates that Hh regulation of OR transport is upstream of *Ci*.

Cos2 Localizes the OR Proteins to the Distal Ciliary Domain

To identify how the Hh pathway regulates OR transport, we next focused on the anterograde cilium transport system, intraflagellar transport complex B (IFT-B). The IFT-B particle is an evolutionarily conserved multiprotein adaptor complex that links cilium cargos to the cilium kinesin II complex (Bhogaraju et al., 2013). IFT88 is a member of the IFT-B complex and is expressed in OSNs (Han et al., 2003). Knockdown of *IFT88* resulted in punctate OR staining at the ciliary base (Figure 4A), showing that OR transport requires the IFT adaptor complex. IFT88 localized to both the cilium base and the cilium compartment in control and *Smo* knockdown flies (Figure 4B), suggesting that the IFT-B complex is not regulated by Hh signaling.

The Hh pathway contains a kinesin-like protein, *Costal2* (*Cos2/Kif7*) in vertebrates, that regulates Ci processing and is required for transport of Smo and, possibly, other cargos (Farzan et al., 2008; Robbins et al., 1997; Sisson et al., 1997; Zadorozny

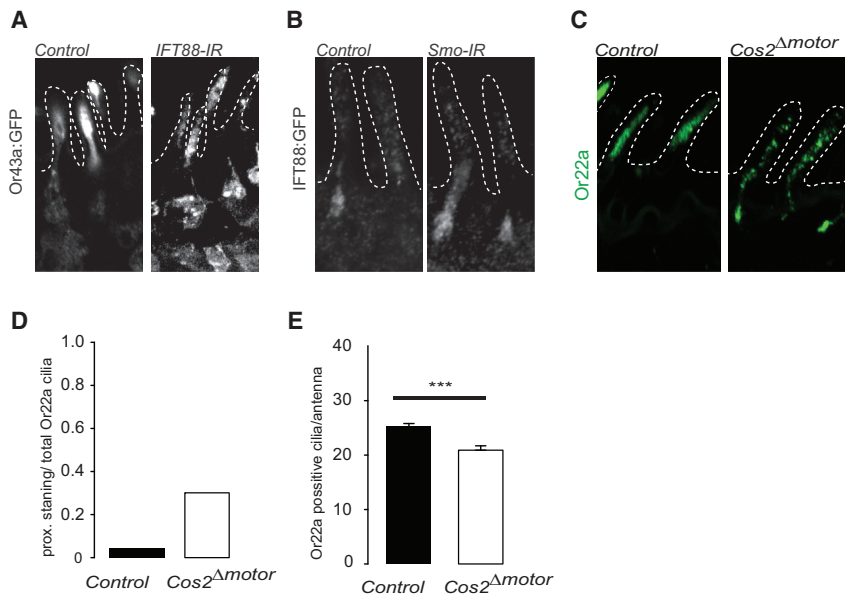


Figure 4. Cos2 Regulates OR Localization to the Distal Cilium Domain

(A) Knockdown of *IFT88* reduces the OSN ciliary Or43a:GFP staining with a marked accumulation at the cilium base. The dotted lines outline the sensilla. (B) *IFT88-IFT88:GFP* is expressed in OSNs, and the fusion protein is localized to the base and cilium in both control and *Smo-IR* flies. (C) Or22a localizes to the proximal cilium segment in *Cos2^{Δmotor}* OSNs. (D) Quantification showing that *Cos2^{Δmotor}* expression (n = 34) increases the fraction of cilia with proximal cilium compartment localization of Or22a (control, n = 36). (E) *Cos2^{Δmotor}* expression reduces the number of Or22a-positive cilia compared with the control (n = 36). ***p < 0.001. Bar graphs show mean ± SEM.

et al., 2015). In addition, Hh regulates Cos2 localization to the cilia (Kuzhandaivel et al., 2014). We therefore hypothesized that Cos2 could be an auxiliary transport system to the IFT-B/kinesin II complex in OSN cilia. Cos2 functions as a dimer, and deletion of the motor domain (*Cos2^{Δmotor}*) generates a dominant-negative version of the protein (Ho et al., 2005). Expression of *Cos2^{Δmotor}* resulted in loss of Or22a-positive cilia (Figure 4E) and mislocalization of Or22a within the cilium compartment (Figure 4C), which shows that Cos2 regulates OR transport into the distal cilium compartment.

DISCUSSION

Here, we demonstrate that the Hh pathway modulates the magnitude of the odorant response in adult *Drosophila*. Our results show that the Hh pathway determines the level of the odorant response because it regulates the response in both the positive and negative directions. Loss of Ptc function increases the odorant response and the risk for long sustained responses, which shows that the Hh pathway limits the response potential of the OSNs and is crucial for maintaining the response at a physiological level. In addition, we show that the OSNs produce Hh protein, which regulates OR localization, which is interesting because autoregulation is one of the prerequisites for an adaptive mechanism. We further show that Hh signaling regulates the responses of OSNs that express different ORs, which demonstrates that the regulation is independent of OSN class and suggests that Hh signaling is a general regulator of the odorant response. It has been shown previously that Hh tunes nociceptive responses in both vertebrates and *Drosophila* (Babcock et al., 2011). It is not yet understood how Hh regulates the level of nociception. However, the regulation is upstream of the nociceptive receptors, which indicates that the Hh pathway is a general regulator of receptor transport and the level of sensory signaling.

Cos2 Regulates OR Cilium Localization

Our results show that OSN cilia have two separate OR transport systems, the Hh-regulated Cos2 and the IFT-B together with the kinesin II system. Our results show that Cos2 is required for OR transport to or within the distal cilium domain and suggest that the IFT system regulates the inflow to the cilium compartment. The two transport systems also are required for Smo cilium localization (Kuzhandaivel et al., 2014). This spatially divided transport of one cargo is similar to the manner in which Kif3a and Kif17 regulate distal and proximal transport in primary cilia in vertebrates (Jenkins et al., 2006). However, Cos2 is not required for the distal location of Orco or tubulin (Kuzhandaivel et al., 2014), indicating that, for some cargos, the IFT system functions in parallel to Cos2.

Interestingly, the vertebrate Cos2 homolog Kif7 organizes the distal compartment of vertebrate primary cilia (He et al., 2014). Similar to our results, Kif7 does so without affecting the IFT system, and its localization to the cilia is dependent on Hh signaling (Endoh-Yamagami et al., 2009; He et al., 2014; Liem et al., 2009). However, the Kif7 kinesin motor function has been questioned (He et al., 2014). Therefore, it will be interesting to analyze whether Kif7-mediated transport of ORs and other transmembrane proteins occurs within the primary cilium compartment and whether the ciliary transport of ORs is also regulated by Hh and Smo signaling in vertebrates. To conclude our results place the already well-studied Hh signaling pathway in the post-developmental adult nervous system and also provide an exciting putative role for Hh as a general regulator of receptor transport to and within cilia.

EXPERIMENTAL PROCEDURES

Drosophila Stocks

The following fly stocks were used: *Pebbled-Gal4* (Jafari et al., 2012) and *UAS-GCAMP5* Bloomington. The *Orco-IR* RNAi line (v13386) was from the Vienna

Drosophila RNAi Center. The following RNAi lines were from the Transgenic RNAi Project: *Hh-IR* (Bloomington stock no. 32489), *Ci-IR* (Bloomington stock no. 31321), and *Smo-IR* (Bloomington stock no. 27037). *UAS-Ci⁷⁵* was a gift from Tom Kornberg. *UAS-Or43a::GFP* was a gift from Leslie Vosshall, and *IFT88-IFT88::GFP* was a gift from Benedicte Durand. The *Or22a-CD8::GFP* (Couto et al., 2005) and *UAS-Smo^{ARR}* (Kuzhandaivel et al., 2014) stocks have been generated previously by us as described.

Behavior Assays

T-maze experiments were performed with 20 3- 5-day-old flies per assay. The flies were starved for 16 hr prior to the experiments, with water provided ad libitum. Apple cider vinegar (100 μ l) was placed in the baited arm with water in the control arm. Flies were counted 10 min after the addition of flies to the maze. The response index was calculated as $(O-C)/T$, where O is the number of flies in the baited arm, C is the number of flies in the control arm, and T is the total number of flies used in the trial. The climbing assay was performed with five flies climbing a 10-cm-long tube, and the percentage of flies at the top 0.5 cm of the tube was determined after 30 s.

Calcium Imaging of the Odorant Responses

Calcium signals from OSNs expressing the calcium sensor GCAMP5 were recorded from intact flies. Four to ten-day-old female virgin flies were anesthetized on ice and glued (Loctite superglue) onto a glass capillary. The antennae were lifted vertically by sticking them to a drop of glue on the head. The preparation was mounted on a micromanipulator, and the fly's head was pushed against a glass coverslip so that at least one of the antennae touched the glass along its longitudinal axis. A drop of water was placed above the coverslip for an immersion objective ($\times 40$, 0.9 numerical aperture [NA], Zeiss Apochromatic). The emitted fluorescence was collected with an electron multiplication (EM) charge-coupled device (CCD) camera (Hamamatsu). A stimulation device (Master 9, AMPI Israel) was used to simultaneously trigger the odorant stimulation, camera, and illumination so that the images were taken at a frequency of 5 Hz with an exposure time of 50 ms. To reduce variability because of photobleaching, the light intensity was kept at 3% in all experiments.

The odorants, ethyl acetate (Sigma-Aldrich, Chemical Abstracts Service [CAS] no. 141-78-6) and methyl octanoate (Sigma-Aldrich, CAS no. 111-11-5), were diluted in mineral oil to reach the nominal concentrations indicated in the corresponding figures (10^{-2} M, with the exception of the dose-response curve in Figure 1C). Apple cider vinegar (50 ml) was poured into 500-ml glass volumetric flasks (Medicinal Air, AGA). The gas was bubbled in water, and the flow rate was set at 100 ml s^{-1} at a pressure of 2 mbar. Solenoid valves switched the air stream between two parallel pathways: one of pure air and another connected to the volumetric flasks containing the odors. In this way, the fly received a constant flow of gas on its antenna of either pure air or air carrying the odorant.

Response Measurements

Imaging was conducted at the focal plane, where the responses were maximal. To quantify odor-evoked responses, we defined a region of interest (ROI) of approximately $15 \mu\text{m}$ surrounding the region of the antenna where the response reached highest intensity, characteristically in the proximal segment of the antenna (Figure 1D). The light intensity inside the ROIs was averaged for each frame, and the peak (usually by the end of the 10-s stimulation period) was used to statistically compare the different groups.

Analysis of the images was conducted using ImageJ software (Schneider et al., 2012).

Immunohistochemistry

The following primary mouse antibodies were used: anti-GFP (1:100), anti-Bruchpilot (1:50, nc82, supernatant, Developmental Studies Hybridoma Bank [DSHB]), and anti Rab11 (1:100, BD Biosciences). The primary rabbit antibodies, anti-GFP (1:2,000, TP-401, Torrey Pines), Lamp1, anti-Rab5, anti-Rab11 (1:100, Abcam), anti-Or22a (1:10,000) and anti-Orco (1:10,000) were gifts from Richard Benton. The secondary antibodies were conjugated to Alexa 488 or Alexa 568 (1:500, Molecular Probes). Antenna immunohistochemistry was performed as described previously (Couto et al., 2005). Or22a images were captured from a subset of stereotypic Or22a sensilla

opposite to the arista. The confocal microscopy images were collected on an LSM 700 (Zeiss) and analyzed on a Zen image browser.

Statistics

The statistical analyses of the cilium counts were performed using the statistical software R (version 3.0.3, The R Core Team). The counts of Or22a-positive cilia and the proportion of positively stained cilium compartments were analyzed by the Poisson and binomial generalized linear models (glms), respectively.

Statistical analyses of the imaging data were performed with GraphPad Prism version 5.00 for Windows (GraphPad, <http://www.graphpad.com>). First, the normal distribution of the data was assessed, and then the groups were compared by one-way ANOVA followed by a Newman-Keuls multiple comparisons test (significance set at 0.05). The data are presented as the mean \pm SEM.

SUPPLEMENTAL INFORMATION

Supplemental Information includes four figures and can be found with this article online at <http://dx.doi.org/10.1016/j.celrep.2015.12.059>.

AUTHOR CONTRIBUTIONS

G.M.S. performed the calcium imaging analysis. L.A. performed the Or22a experiments. E.H. performed the Cos2 and Ci experiments. S.W.S. performed the OR vesicle experiments. A.K. and S.J. performed the behavior experiments. B.G. and M.A. wrote the paper.

ACKNOWLEDGMENTS

We thank Leslie Vosshall, Thomas Kornberg, Benedicte Durand, and Matthew Scott for flies; Richard Benton for reagents; Olivia Forsberg and Johanna Karlsson for excellent technical assistance; Carlos Ribeiro and Staffan Bohm for discussions and comments on the manuscript; and Sarah Lindström for excellent English editing. This work was supported by the Swedish Foundation for Strategic Research (Grant F06-0013).

Received: July 29, 2015

Revised: October 26, 2015

Accepted: December 10, 2015

Published: January 7, 2015

REFERENCES

- Aza-Blanc, P., Ramirez-Weber, F.A., Laget, M.P., Schwartz, C., and Kornberg, T.B. (1997). Proteolysis that is inhibited by hedgehog targets *Cubitus interruptus* protein to the nucleus and converts it to a repressor. *Cell* 89, 1043–1053.
- Babcock, D.T., Shi, S., Jo, J., Shaw, M., Gutstein, H.B., and Galko, M.J. (2011). Hedgehog signaling regulates nociceptive sensitization. *Curr. Biol.* 21, 1525–1533.
- Benton, R., Sachse, S., Michnick, S.W., and Vosshall, L.B. (2006). Atypical membrane topology and heteromeric function of *Drosophila* odorant receptors in vivo. *PLoS Biol.* 4, e20.
- Bhogaraju, S., Engel, B.D., and Lorentzen, E. (2013). Intraflagellar transport complex structure and cargo interactions. *Cilia* 2, 10.
- Briscoe, J., and Théron, P.P. (2013). The mechanisms of Hedgehog signalling and its roles in development and disease. *Nat. Rev. Mol. Cell Biol.* 14, 416–429.
- Corbit, K.C., Aanstad, P., Singla, V., Norman, A.R., Stainier, D.Y., and Reiter, J.F. (2005). Vertebrate Smoothed functions at the primary cilium. *Nature* 437, 1018–1021.
- Couto, A., Alenius, M., and Dickson, B.J. (2005). Molecular, anatomical, and functional organization of the *Drosophila* olfactory system. *Curr. Biol.* 15, 1535–1547.
- DeMaria, S., and Ngai, J. (2010). The cell biology of smell. *J. Cell Biol.* 191, 443–452.

- Denef, N., Neubüser, D., Perez, L., and Cohen, S.M. (2000). Hedgehog induces opposite changes in turnover and subcellular localization of patched and smoothened. *Cell* *102*, 521–531.
- Dobritsa, A.A., van der Goes van Naters, W., Warr, C.G., Steinbrecht, R.A., and Carlson, J.R. (2003). Integrating the molecular and cellular basis of odor coding in the *Drosophila* antenna. *Neuron* *37*, 827–841.
- Endoh-Yamagami, S., Evangelista, M., Wilson, D., Wen, X., Theunissen, J.W., Phamluong, K., Davis, M., Scales, S.J., Solloway, M.J., de Sauvage, F.J., and Peterson, A.S. (2009). The mammalian *Cos2* homolog *Kif7* plays an essential role in modulating Hh signal transduction during development. *Curr. Biol.* *19*, 1320–1326.
- Farzan, S.F., Ascano, M., Jr., Ogden, S.K., Sanial, M., Brigui, A., Plessis, A., and Robbins, D.J. (2008). *Costal2* functions as a kinesin-like protein in the hedgehog signal transduction pathway. *Curr. Biol.* *18*, 1215–1220.
- Fishilevich, E., and Vosshall, L.B. (2005). Genetic and functional subdivision of the *Drosophila* antennal lobe. *Curr. Biol.* *15*, 1548–1553.
- Galizia, C.G., Münch, D., Strauch, M., Nissler, A., and Ma, S. (2010). Integrating heterogeneous odor response data into a common response model: A DoOR to the complete olfactome. *Chem. Senses* *35*, 551–563.
- Goetz, S.C., and Anderson, K.V. (2010). The primary cilium: a signalling centre during vertebrate development. *Nat. Rev. Genet.* *11*, 331–344.
- Hallem, E.A., and Carlson, J.R. (2006). Coding of odors by a receptor repertoire. *Cell* *125*, 143–160.
- Han, Y.G., Kwok, B.H., and Kernan, M.J. (2003). Intraflagellar transport is required in *Drosophila* to differentiate sensory cilia but not sperm. *Curr. Biol.* *13*, 1679–1686.
- He, M., Subramanian, R., Bangs, F., Omelchenko, T., Liem, K.F., Jr., Kapoor, T.M., and Anderson, K.V. (2014). The kinesin-4 protein *Kif7* regulates mammalian Hedgehog signalling by organizing the cilium tip compartment. *Nat. Cell Biol.* *16*, 663–672.
- Ho, K.S., Suyama, K., Fish, M., and Scott, M.P. (2005). Differential regulation of Hedgehog target gene transcription by *Costal2* and *Suppressor of Fused*. *Development* *132*, 1401–1412.
- Ingham, P.W., Nakano, Y., and Seger, C. (2011). Mechanisms and functions of Hedgehog signalling across the metazoa. *Nat. Rev. Genet.* *12*, 393–406.
- Jafari, S., Alkhori, L., Schleiffer, A., Brochtrup, A., Hummel, T., and Alenius, M. (2012). Combinatorial activation and repression by seven transcription factors specify *Drosophila* odorant receptor expression. *PLoS Biol.* *10*, e1001280.
- Jana, S.C., Girotra, M., and Ray, K. (2011). Heterotrimeric kinesin-II is necessary and sufficient to promote different stepwise assembly of morphologically distinct bipartite cilia in *Drosophila* antenna. *Mol. Biol. Cell* *22*, 769–781.
- Jenkins, P.M., Hurd, T.W., Zhang, L., McEwen, D.P., Brown, R.L., Margolis, B., Verhey, K.J., and Martens, J.R. (2006). Ciliary targeting of olfactory CNG channels requires the CNGB1b subunit and the kinesin-2 motor protein, KIF17. *Curr. Biol.* *16*, 1211–1216.
- Knödler, A., Feng, S., Zhang, J., Zhang, X., Das, A., Peränen, J., and Guo, W. (2010). Coordination of Rab8 and Rab11 in primary ciliogenesis. *Proc. Natl. Acad. Sci. USA* *107*, 6346–6351.
- Kuzhandaivel, A., Schultz, S.W., Alkhori, L., and Alenius, M. (2014). Cilia-mediated hedgehog signaling in *Drosophila*. *Cell Rep.* *7*, 672–680.
- Liem, K.F., Jr., He, M., Ocbina, P.J., and Anderson, K.V. (2009). Mouse *Kif7/ Costal2* is a cilia-associated protein that regulates Sonic hedgehog signaling. *Proc. Natl. Acad. Sci. USA* *106*, 13377–13382.
- Méthot, N., and Basler, K. (1999). Hedgehog controls limb development by regulating the activities of distinct transcriptional activator and repressor forms of *Cubitus interruptus*. *Cell* *96*, 819–831.
- Ohlmeyer, J.T., and Kalderon, D. (1997). Dual pathways for induction of wingless expression by protein kinase A and Hedgehog in *Drosophila* embryos. *Genes Dev.* *11*, 2250–2258.
- Robbins, D.J., Nybakken, K.E., Kobayashi, R., Sisson, J.C., Bishop, J.M., and Théron, P.P. (1997). Hedgehog elicits signal transduction by means of a large complex containing the kinesin-related protein *costal2*. *Cell* *90*, 225–234.
- Rohatgi, R., and Scott, M.P. (2007). Patching the gaps in Hedgehog signalling. *Nat. Cell Biol.* *9*, 1005–1009.
- Schneider, C.A., Rasband, W.S., and Eliceiri, K.W. (2012). NIH Image to ImageJ: 25 years of image analysis. *Nat. Methods* *9*, 671–675.
- Sisson, J.C., Ho, K.S., Suyama, K., and Scott, M.P. (1997). *Costal2*, a novel kinesin-related protein in the Hedgehog signaling pathway. *Cell* *90*, 235–245.
- Teperino, R., Aberger, F., Esterbauer, H., Riobo, N., and Pospisilik, J.A. (2014). Canonical and non-canonical Hedgehog signalling and the control of metabolism. *Semin. Cell Dev. Biol.* *33*, 81–92.
- Vosshall, L.B., and Stocker, R.F. (2007). Molecular architecture of smell and taste in *Drosophila*. *Annu. Rev. Neurosci.* *30*, 505–533.
- Wang, J., and Deretic, D. (2015). The Arf and Rab11 effector FIP3 acts synergistically with ASAP1 to direct Rabin8 in ciliary receptor targeting. *J. Cell Sci.* *128*, 1375–1385.
- Zadorozny, E.V., Little, J.C., and Kalderon, D. (2015). Contributions of *Costal 2-Fused* interactions to Hedgehog signaling in *Drosophila*. *Development* *142*, 931–942.